AUTHOR'S POST PRINT (Romeo Colour: Green)
MSSU: Microgravity & Space Station Utilization (ISSN: 0958-5036), 3 (4): 51-62 (2002).
Publisher version available at
http://www.liguori.it/periodici.asp?cod_collana=201

WELL-POSED PROBLEMS FOR THE NAVIER-STOKES EQUATIONS IN THE MICROGRAVITY ENVIRONMENT

Marcello Lappa

Via Salvator Rosa 53, San Giorgio a Cremano, 80046, Napoli, Italy, Fax: +39-81-6042100 and
MARS (Microgravity Advanced Research and Support Center) Via Gianturco 31 - 80146, Napoli, Italy,
Current e-mail address: marcello.lappa@strath.ac.uk, marlappa@unina.it

Abstract - This article is devoted to a critical and concise analysis of the different types of convection that can arise in the microgravity environment. A significant effort is provided to illustrate their genesis, the governing non-dimensional parameters, the scaling properties as well as some critical requirements that must be taken into account when trying to simulate these convective flows by means of numerical computations. Along these lines, most of the discussion is devoted to introduce and elucidate some aspects, often undervalued and overlooked by researchers, that are of paramount importance for obtaining "well-posed problems" from a theoretical, mathematical and computational point of view as well as for the physical consistency and relevance of the results.

1. INTRODUCTION

Gravity dominates everything on Earth, from the way life has developed to the way materials interact. But aboard a spacecraft orbiting the Earth, the effects of gravity are barely felt. In this "microgravity environment", scientists can conduct experiments that are all but impossible to perform on Earth. In this virtual absence of gravity as we know it, space flight gives scientists a unique opportunity to study the states of matter (solids, liquids and gases), and the forces and processes that affect them.

In practice, microgravity or near-weightlessness corresponds to a free-fall situation and in this condition various phenomena are significantly altered, in particular convection, buoyancy, hydrostatic pressure and sedimentation. When microgravity conditions are attained, fluids do "incredible" things.

Scientific disciplines affected include fluid physics and transport phenomena, combustion, crystal growth and solidification, biological processes and biotechnology.

Microgravity is instrumental in unraveling processes that are interwoven or overshadowed in normal gravity. It can therefore be regarded as an important tool for improving models of complex phenomena and hence manufacturing processes on Earth (Rogers et al. [1]). Critical knowledge gained from microgravity experiments, in fact, is validating new, more complex models, accelerating the current trend towards predictable and reproducible phenomena, and enabling the development of new industrial processes (i.e. a commercial return from space research activities based on the application on the ground of the knowledge obtained in space).

Within this context the present article develops working engineering models that can be easily employed in applications, while providing a rigorous mathematical and numerical framework for deeper understanding and effective treatment of phenomena encountered in microgravity and/or unmasked by this environment.

Mathematical modeling is the art and craft of building a system of equations that is both sufficiently complex to do justice to physical reality and sufficiently simple to focus on the most significant aspects of the given situation. Numerical simulation is the art of solving these equations. Numerical methods are important since they are a decisive tool to reduce the number of expensive space experiments. They are propaedeutical to plan and improve the experimental set-ups and to optimize the new production techniques suggested by the amount of knowledge obtained in space.

Superimposed on this is the fact that most of the scientists carrying out research on Earth (as well as the undergraduate and the Ph.D. students) cannot directly access microgravity platforms. For this reason the use of numerical computations is of paramount importance (often it is the only way) for the investigation of the properties of materials and fluids in the zero-g (simulated) environment, for the understanding of forces and processes affecting them (hidden or undervalued in normal gravity) and finally for the design of the aforementioned new manufacturing methods to be used on Earth.

However, numerical simulation requires special care for a number of aspects that must be properly evaluated and taken into account in order to deal with problems "well posed" from a theoretical, mathematical and computational point of view.

This paper gains "critical" information from fifty of the author's relevant and recent papers to illustrate the philosophy of modeling, the practical applications and some insights into the physics. It is conceived in order to be a useful reference guide for other specialists in these disciplines as well as an advanced level paper for

students taking part in courses on CFD (computational fluid-dynamics), or on numerical methods for materials engineering and similar techniques. It is directed at readers already engaged or starting to be engaged in these topics. Engineers, designers and students will find the necessary numerical techniques and the revealing insights into some aspects still poorly known or understood.

The paper runs as follow: Section 2 briefly introduces the mathematical models and the common approximations that have enjoyed a widespread use over the last years for the simulation of convective flows arising in the microgravity environment; Section 3 is devoted to a critical comparison of the different available methods based on the original or equivalent forms of the Navier-Stokes equations; the last part of the study focuses on the numerical treatment of boundary layers and/or viscous/vorticity singularities too often ignored or not properly considered in the literature.

2. MATHEMATICAL MODELS

2.1 BUOYANCY CONVECTION AND THE BOUSSINESQ MODEL

In the presence of steady gravity (on the ground conditions $g=g_o$ or steady acceleration levels on microgravity platforms) the velocity, temperature and concentration fields in the considered fluid can be determined by the differential balance equations (for mass, momentum, energy and mass species).

Following the usual Boussinesq approximation for incompressible fluids (see, e.g., Fletcher, [2]), the physical properties are assumed constant except the density ρ in the driving force appearing in the momentum equation (see eq. (2b) below), which is assumed to be a linear function of temperature and concentration :

$$\rho = \rho_0 \left[1 + \beta_T (T - T_0) + \beta_c (C - C_0)\right] \tag{1}$$

where β_T and β_C are the thermal and solutal expansion coefficients respectively, T_o and C_o reference values for temperature and concentration respectively.

The equations in dimensional form read:

$$\underline{\nabla} \cdot \underline{V} = 0 \tag{2a}$$

$$\frac{\partial \underline{V}}{\partial t} + \underline{\nabla} \cdot \left[\underline{V}\,\underline{V}\right] + \frac{1}{\rho_0} \underline{\nabla} p = \nu \nabla^2 \underline{V} - \left[\beta_T (T - T_0) + \beta_c (C - C_0)\right] \underline{g} \tag{2b}$$

$$\frac{\partial T}{\partial t} + \underline{\nabla} \cdot \left[\underline{V} T\right] = \alpha \nabla^2 T \tag{3a}$$

$$\frac{\partial C}{\partial t} + \underline{\nabla} \cdot \left[\underline{V} C\right] = D \nabla^2 C \tag{3b}$$

where V is the velocity field, T the temperature, C the concentration and p the pressure (ν is the kinematic viscosity, α is the thermal diffusivity and D is the species diffusion coefficient). The identification of the relevant parameters in the momentum and energy (or specie) equations requires that these equations are posed in non-dimensional form through the choice of relevant reference quantities.

Thermogravitational convection

In the case of thermal problems (solutal effects absent) usually the non-dimensional form results from scaling the lengths by a reference distance (L) and the velocity by the energy diffusion velocity $V_d = V_\alpha = \alpha/L$; the scales for time and pressure are, respectively, L^2/α and $\rho\alpha^2/L^2$. The temperature, measured with respect to T_o, is scaled by ΔT (reference temperature gradient). This approach leads to:

$$\underline{\nabla} \cdot \underline{V} = 0 \tag{4}$$

$$\frac{\partial \underline{V}}{\partial t} = -\underline{\nabla} p - \underline{\nabla} \cdot \left[\underline{V}\,\underline{V}\right] + \mathrm{Pr}\ \nabla^2 \underline{V} - \mathrm{Pr} \cdot Ra\ T\ \underline{i}_g \tag{5}$$

$$\frac{\partial T}{\partial t} = -\underline{\nabla} \cdot \left[\underline{V} T\right] + \nabla^2 T \tag{6}$$

and the relevant non-dimensional numbers are the well known Prandtl and Rayleigh numbers

$$\mathrm{Pr} = \frac{\upsilon}{\alpha} \tag{7}$$

$$Ra = \frac{g \beta_T \Delta T L^3}{\upsilon \alpha} \tag{8}$$

Where the Rayleigh number also measures the magnitude of the buoyancy velocity V_g to the thermal diffusive velocity, where V_g reads

$$V_g = \frac{g \beta_T \Delta T (L)^2}{\nu} \tag{9}$$

Moreover

$$Gr = Ra / \mathrm{Pr} = \frac{g \beta_T \Delta T L^2}{\upsilon^2} \tag{10}$$

is the Grashof number which represents the ratio of buoyant to molecular thermal transport (only two of the Gr, Ra and Pr numbers are independent) .

Solutogravitational convection

In the case of compositionally inhomogeneous liquids (solutal problems) usually the non-dimensional form results from scaling the lengths by a reference distance (L) and the velocity by the solute diffusion velocity $V_d = V_D = D/L$; the scales for time and pressure are, respectively, L^2/D and $\rho D^2/L^2$. The concentration, measured with respect to C_o, can be scaled by its initial value (i.e. $C = (C_{dim} - C_o)/C_o$). This approach leads to

$$\underline{\nabla} \cdot \underline{V} = 0 \tag{11}$$

$$\frac{\partial \underline{V}}{\partial t} = -\underline{\nabla} p - \underline{\nabla} \cdot \left[\underline{V}\,\underline{V}\right] + Sc\ \nabla^2 \underline{V} - Sc \cdot Ra\ C\ \underline{i}_g \tag{12}$$

$$\frac{\partial C}{\partial t} = -\underline{\nabla} \cdot \left[C T\right] + \nabla^2 C \tag{13}$$

and the relevant non-dimensional numbers are

$$Sc = \frac{\upsilon}{D} \tag{14}$$

$$Ra = \frac{g\beta_c C_o L^3}{\upsilon D} \tag{15}$$

where the solutal Rayleigh number measures the magnitude of the buoyancy velocity V_g to the solutal diffusive velocity, where V_g reads

$$V_g = \frac{g\beta_C C_O (L)^2}{\nu} \tag{16}$$

Moreover

$$Gr = Ra / Sc = \frac{g\beta_C C_O L^2}{D^2} \tag{17}$$

is the Grashof number which in this case represents the ratio of buoyant to molecular transport (i.e. diffusion) of solute. Note that in practice to obtain a reliable estimation of the order of magnitude of the buoyancy velocity the effective concentration gradient ΔC driving the solutal flow should be used in place of C_o in eq. (16).

2.2 SOME ASPECTS OF MARANGONI FLOW

Microgravity gives the possibility to avoid some limitations related to the ground environment, e.g. the aforementioned buoyancy driven convection that is the most important causes of imperfections and defects in crystals and materials grown by a number of techniques. Moreover in zero-g conditions it is possible to form very large floating liquid volumes. Such floating configurations are often used for processes that benefit from the absence of containers (the absence of contact with solid walls, in fact, prevents contaminations and other undesired effects). During recent years, the availability of sounding rockets and orbiting laboratories as the Spacelab, has made possible, in fact, microgravity experiments and manufacturing processing with large melt/air surfaces, which could not be performed on Earth under normal gravity conditions.

However, the presence of the aforementioned free-melt-gas interfaces at different temperatures (an intrinsic consequence of the solidification processes), that in many cases offers a number of advantages in terms of final purity of the materials, induces another type of undesired flow, the so-called Marangoni convection. This convective flow is basically a surface tension-driven and gravity-independent phenomenon. The text below provides the necessary mathematical models.

The surface tension σ for many cases of practical interest exhibits a linear dependence on temperature and concentration:

$$\sigma = \sigma_o - \sigma_T (T - T_o) - \sigma_c (C - C_o) \tag{18}$$

where σ_o is the surface tension for $T=T_o$ and $C=C_o$, $\sigma_T=-d\sigma/dT>0$ (σ is a decreasing function of T) and $\sigma_c=-d\sigma/dC$.

If a non-isothermal free surface is involved in the considered process (for instance metal solidification), then surface tension forces $\underline{\nabla}_S\sigma$ ($\underline{\nabla}_S$ derivative tangential to the interface) arise that must be balanced by viscous stresses in the liquid $\underline{S}\cdot\underline{n}$ ($\underline{n}$ unit vector perpendicular to the free interface, $\underline{S}$ stress tensor). This balance yields:

$$\mu \frac{\partial \underline{V}}{\partial n} = -\sigma_T \underline{\nabla}_S T \tag{19}$$

and in non-dimensional form (scaling the lengths by a reference distance L, the velocities by the energy diffusion velocity and the temperature by the aforementioned reference ΔT):

$$\frac{\partial \underline{V}}{\partial n} = -Ma\ \underline{\nabla}_S T \tag{20}$$

where $Ma = \sigma_T \Delta T L/\mu\alpha$ (μ being the dynamic viscosity) is the so-called Marangoni number. This condition enforces a flow by tangential variation of the surface tension. The motion immediately results whenever a temperature gradient exists, no matter how small (thermocapillary convection). The surface moves from the region with a low surface tension to that with a high surface tension, dragging the nearby fluid with it by viscous forces.

Prior to the space program, this phenomenon had been ignored in investigations of materials processing on Earth. In microgravity, the reduced level of buoyancy-driven convection allowed Marangoni convection to become obvious. Once it became recognized, it was found to be significant in some Earth-based processes as well.

The following non-dimensional numbers are of particular importance (see, e.g., Kuhlmann [3]):

$$\mathrm{Pr} = \frac{\upsilon}{\alpha} \tag{21}$$

$$\mathrm{Re} = \frac{\sigma_T \Delta T L}{\rho \upsilon^2} \tag{22}$$

$$Ca = \frac{\sigma_T \Delta T}{\sigma_O} \tag{23}$$

$$Ma = \mathrm{Re}\cdot\mathrm{Pr} = \frac{\sigma_T \Delta T L}{\mu\alpha} \tag{24}$$

The Reynolds number (Re) measures the magnitude of the tangential stress $\sigma_T\Delta T/L$ to the viscous stress $\rho\nu^2/L^2$; the Prandtl number (Pr) measures the rate of momentum diffusion ν to that of heat diffusion α, and the Marangoni number is $Ma=Re\cdot Pr$. Only two of these three numbers are independent.

The capillary number ($Ca=Re\cdot Oh$, $Oh=\rho\nu^2/\sigma_0 L$ being the Ohnesorge number) gives the relative change of the surface tension due to temperature variations. It involves the mean surface tension σ_0 and it is an important measure of the dynamic deformability of the free surface. The interface location is determined, in fact, by the hydrodynamic and the Laplace pressure. The relative importance of both is given by the ratio of the relative magnitudes ($\sigma_T\ \Delta T/L$) and σ_o/L. This ratio is the above-mentioned capillary number $Ca= \sigma_T\ \Delta T/\sigma_o$. If $Ca\rightarrow 0$

(i.e. Ca<<1) the dynamic surface deformation can be neglected.
Features of interest are the fundamental scales of velocity and temperature that determine the strength of the flow.
It has been noted by Rybicki and Florian [4] that the appropriate scaling of the dimensional velocity is the Marangoni velocity:

$$V_{Ma}^{T} = \frac{\sigma_T \Delta T}{\mu} \tag{25}$$

Then the Marangoni number can also be seen as the measure of the relative importance of the Marangoni and of the thermal diffusion velocities.
Moreover for small Reynolds and Prandtl numbers the temperature field scales like Re·Pr·ΔT.
In many situations, the capillary number is small and the flow induced surface deformations can be expanded in a power series of Ca to yield the leading order surface deflection δ_o, which turns out to be of O(Ca·L).
To summarize the scaling for small Re, Pr and Ca read:

$$V = O\left(\frac{\sigma_T \Delta T}{\mu}\right) \tag{26}$$

$$\varepsilon_T = \max(T - T_d) = O(Re \cdot Pr \cdot \Delta T) = O(Ma \cdot \Delta T) \tag{27}$$

$$\delta_o = O(Ca \cdot L) \tag{28}$$

where T_d is the reference diffusive temperature field (i.e. the temperature distributions that would be established in absence of convection) and ε_T is the corresponding temperature disturbance.
According to eq. (18) Marangoni convection can arise also as a consequence of concentration gradients; in this case it is usually referred to as "solutocapillary" convection.

3. SOLUTION OF THE INCOMPRESSIBLE NAVIER-STOKES EQUATIONS

3.1 VORTICITY METHODS

In some cases equivalent forms of the momentum equation (i.e. equivalent in the continuum, but generally not equivalent when spatially discretized) can be used to advantage. These alternative equations are all derived from the "primitive" equation from differentiation (in part) and often after additional insights regarding incompressible flow. They are also often used as the starting point for generating alternative numerical solution methods (Gresho [5]).
For instance for two-dimensional cases, stream function-vorticity (ψ-ζ) methods have enjoyed a widespread use during the last years owing to computational efficiency and simplicity. The major advantage of these method relies on the possibility to solve the equations leaving aside problems related to the pressure gradient that is usually regarded as a "strange" object by numerical investigators. For the same reason velocity-vorticity methods have been also used for three-dimensional problems. In such methods the presence of the pressure gradient is removed through application of the curl operator to the momentum equation (the curl of the gradient of a scalar quantity, in fact, is zero). Applying the curl operator and using the fact that both $\underline{V}$ and $\underline{\omega} = \underline{\nabla} \wedge \underline{V}$ are div-free:

$$\frac{\partial \underline{\omega}}{\partial t} + \underline{V} \cdot \underline{\nabla}\underline{\omega} = \underline{\omega} \cdot \underline{\nabla}\underline{V} + \Pr \ \nabla^2 \underline{\omega} + \underline{\nabla} \wedge \underline{F}_g \tag{29a}$$

where $\underline{F}_g$ takes into account gravity (steady or oscillatory) forces.
Furthermore, the curl of $\underline{\nabla} \wedge \underline{V} = \underline{\omega}$ leads to another higher order equation, a Poisson equation for the velocity:

$$\nabla^2 \underline{V} = -\underline{\nabla} \wedge \underline{\omega} \tag{29b}$$

that is still a kinematic equation. These two equations are at the basis of velocity-vorticity formulations (see, e.g., Farouk and Fusegi [6]).
Some numerical investigators have also tried an approach based on the introduction of the 3D stream function defined as

$$\underline{\nabla} \wedge \underline{\Psi} = \underline{V} \tag{30a}$$

known as the so-called 3D vorticity/vector-vorticity formulation. Accordingly the dimensionless equations governing the evolution of $\underline{\omega}$ and $\underline{\Psi}$ are eq. (29a) and (30b) respectively:

$$\underline{\nabla} \wedge \underline{\nabla} \wedge \underline{\Psi} = \underline{\omega} \tag{30b}$$

These methods on the one hand have enjoyed a reasonable success for the aforementioned reasons but on the other hand have been characterized by some conceptual difficulties mainly coming from a non-complete knowledge of the boundary conditions making the problem well-posed from a computational/theoretical point of view (Gresho [5]).

3.2 PRIMITIVE VARIABLES METHODS

A different class of methods not needing mathematical manipulation and transformation (i.e. the introduction of the vorticity through application of the curl operator), however, has been simultaneously developed. In such class the pressure gradient is not eliminated. Rather it is used for introducing (with the aid of the continuity equations) an additional equation that leads to a closed set of equations. The major advantage offered by this class of methods (see, e.g., the MAC method introduced by Harlow and Welch [7]) relies on the possibility to solve the problem directly in terms of the primitive variables (i.e. velocity and pressure) of the fluid. Superimposed on this, the problem related to the boundary conditions that make the problem well posed has been investigated to a certain extent leading to widely recognized theoretical results (Gresho and Sani [8]).

For instance forward differences in time can be used to discretize the partial differential equations in their primitive variable form (of course this is only an example used herein for the convenience of the reader, usually high order temporal schemes should be used to obtain reliable accuracy), obtaining:

$$\underline{V}^{n+1} = \underline{V}^{n} + \Delta t\left[-\underline{\nabla}\cdot(\underline{V}\underline{V}) + \mathrm{Pr}\ \nabla^2\ \underline{V}\right]^n - \Delta t\underline{\nabla}p^n\ + \Delta t\underline{F}_g^n$$

$\rightarrow$

$$\underline{V}^{n+1} = \underline{R}(\underline{V}^n) - \Delta t\underline{\nabla}p^n \tag{31}$$

where the operator $\underline{\mathrm{R}}$ reads

$$\underline{R}(\underline{V}) = \underline{V} + \Delta t\left[-\underline{\nabla}\cdot(\underline{V}\underline{V}) + \mathrm{Pr}\ \nabla^2\ \underline{V}\right] + \Delta t\underline{F}_g^n$$

(n superscript denotes time step).

The pressure field can be computed by solving a Poisson equation resulting from the divergence of the momentum equation with the help of the continuity equation $\underline{\nabla}\cdot\underline{V}^{n+1} = 0$:

$$\nabla^2 \mathrm{p}^{\mathrm{n}} = \frac{1}{\Delta \mathrm{t}}\underline{\nabla}\cdot\underline{R}^n \tag{32}$$

This formulations requires (for retaining coherence with respect to eq. (32) i.e. for obtaining a well-posed problem) that at the physical boundaries of the computational domain the pressure satisfies conditions obtained projecting the operator $\underline{\mathrm{R}}$ along the direction perpendicular to the boundary itself i.e.:

$$\frac{\partial P}{\partial n} = \frac{1}{\Delta \mathrm{t}}\underline{R}\cdot\underline{n} \tag{33}$$

$\underline{\mathrm{n}}$ being the unit vector pointing into the liquid domain.

Gresho and Sani [8] in particular were the first to demonstrate that the proper boundary condition (BC) is simply the Neumann BC obtained by applying the normal component of the momentum equation on the frontier of the domain (i.e. eq. (33)) because this is the only BC that can always assure that $\underline{\nabla}\cdot\underline{V} = 0$ in the domain.

Subtracting the Poisson equation from the divergence of the momentum equation it reads:

$$\frac{\partial(\underline{\nabla}\cdot\underline{V})}{\partial t} = 0 \tag{34}$$

this equation is important since it shows that $\underline{\nabla}\cdot\underline{V} = 0$ remains zero in the computational domain if it is zero at the initial instant i.e. $\underline{\nabla}\cdot\underline{V}_o = 0$.

Eqs. (31-32) can be used for a time-marching procedure where p^{n} is computed as function of $\underline{\mathrm{V}}^{\mathrm{n}}$ (eq. (32)) and $\underline{\mathrm{V}}^{\mathrm{n+1}}$ is computed as a function of $\underline{\mathrm{V}}^{\mathrm{n}}$ and p^{n} (eq. (31). This approach was referred to as the Consistent pressure Poisson equation CPPE in Gresho and Sani [8]. If this CPPE formulation is employed and the initial velocity field is div-free, according to eq. (34) the solution will be div-free for all time.

On the contrary, the initial condition for vorticity formulations is poorly understood: there are no constraints and therefore the problem is often ill-posed (Gresho [5]). There are no BCs on the vorticity, but the value (which is often poorly behaved) of the vorticity on the boundary does play a major role in most vorticity-based methods. Whereas vortex sheets are little more than a minor inconvenience in primitive variable formulations, they are often the principal focus of attention in vorticity-based methods, partly because they are computationally cumbersome.

Vorticity is a challenging variable to compute. Usually more grid points are needed in the boundary layer with a vorticity method with respect to a primitive variables method to get the same accuracy.

Some difficulties arise, however, also with the primitive variable formulation due to the complexity of the operator $\underline{\mathrm{R}}$ that requires demanding manipulations for spatial discretization. For this reason a simplified variation has been proposed, the so-called SMAC method. Among other things this method also allows one to impose homogeneous boundary conditions for the pressure rather than the complex non-homogeneous ones (33).

The SMAC method for the solution of the incompressible Navier-Stokes equations proceeds as a type of fractional step method by first writing a modified momentum equation and then updating the velocity field using the computed pressure to account for the continuity equation. More precisely, at each time step, an intermediate velocity field $\underline{\mathrm{V}}^*$ is found without the knowledge of the correct pressure field, and therefore no incompressibility condition is enforced. The intermediate velocity field is then corrected by a second step in which a pressure equation is solved and then the computed pressure is used to produce a divergence-free velocity field.

In practice, according to the SMAC method, the computation of the velocity field at each time step is split into two sub-steps. In the first, an approximate velocity field $\underline{\mathrm{V}}^*$ corresponding to the correct vorticity of the field, but with $\underline{\nabla}\cdot\underline{V}^* \neq 0$, is computed at time (n+1) neglecting the pressure gradient in the momentum equation, i.e.,

$$\underline{V}^* = \underline{V}^n + \Delta t\left[-\underline{\nabla}\cdot(\underline{V}\underline{V}) + \mathrm{Pr}\ \nabla^2\underline{V}\right]^n + \Delta t\underline{F}_g^n \tag{35}$$

In the second sub-step, the pressure field is computed by solving a Poisson equation obtained imposing that $\underline{\nabla}\cdot\underline{V}^{n+1} = 0$:

$$\nabla^2 \mathrm{p}^{\mathrm{n}} = \frac{1}{\Delta \mathrm{t}}\underline{\nabla}\cdot\underline{V}^* \tag{36}$$

Finally, the velocity field is updated using the computed pressure field to account for continuity:

$$\underline{\mathrm{V}}^{\mathrm{n+1}} = \underline{\mathrm{V}}^* - \Delta \mathrm{t}\underline{\nabla}\,\mathrm{p}^{\mathrm{n}} \tag{37}$$

If the effective velocity boundary conditions are used for the solution of eq. (35) then $\underline{V}^*$ need not to be corrected on the boundary (i.e. $\underline{V}^{n+1} = \underline{V}^*$); this leads to homogeneous boundary conditions for the pressure equation, i.e.

$$\frac{\partial P}{\partial n} = 0 \tag{38}$$

By comparison of eqs. (32) and (36) and (33) and (38) it is evident how the SMAC methods introduces significant simplifications with respect to the MAC formulation without sacrificing accuracy or well-posed conditions.

In practice this method makes use of the Hodge decomposition theorem, which states that any vector function $\underline{V}$ can be decomposed into a divergence-free part $\underline{V}^*$ plus the gradient of a scalar potential $\Re$, i.e. $\underline{V} = \underline{V}^* + \underline{\nabla}\Re$ where for the SMAC method $\underline{\nabla}\Re = -\underline{\nabla}p/\Delta t$. Accordingly the quantity p in eq. (36) is often called pseudo-pressure to distinguish it with respect to the physical pressure that can be obtained solving eq. (32). If the physical pressure is needed eq. (32) still must be solved with the BC (33) when the SMAC formulations is used.

The Poisson equation (36) is an elliptic equation and can be solved with a SOR (Successive Over Relaxation) iterative method. Eq. (35) is instead a parabolic equation and can be solved using explicit or implicit schemes (the use of explicit schemes is recommended in the present article since they facilitate a parallel implementation of the code based on a grid partition strategy, see, e.g., Lappa [9] and Lappa and Savino [10] for further details).

Also, the species and energy equations are parabolic in nature (T or C at time n+1 can be simply computed as a function of the fields a time n):

$$T^{n+1} = T^n + \Delta t\left[-\underline{\nabla}\cdot(\underline{V}T) + \nabla^2 T\right]^n \tag{39}$$

If g-jitter are present and their properties (in terms of frequency and amplitude) fall within the range of applicability of the Gershuni's formulations [11-13], the source term in the momentum equation reads:

$$\underline{F}_g^n = \mathrm{Pr}\cdot Ra_V\left[(\underline{w}\cdot\underline{\nabla}T)\underline{n} - \underline{w}\cdot\underline{\nabla}\underline{w}\right]^n \tag{40}$$

where the auxiliary potential function $\underline{w}$ must be obtained solving the equation:

$$\underline{\nabla}^2\underline{w}^n = -\underline{\nabla}\wedge\left(\underline{\nabla}T^n\wedge\underline{n}\right) \tag{41}$$

(that is elliptic in nature and can be solved with the same numerical procedures used for eq. (36)) and Ra_v is the vibrational Rayleigh number $Ra_V = \frac{(b\omega\beta_T\Delta TL)^2}{2\nu\alpha}$, where b is the amplitude and f=ω/2π is the frequency of the g-jitter disturbance $\underline{s}(t) = \mathrm{bsin}(\omega\ \mathrm{t})\ \underline{n}$.

Many operations on spacecraft cause vibrations of the vehicle and the payloads. These vibrations are often referred to as "g-jitters" because their effects are similar to those that would be caused by a time-varying gravitational field. Typical sources for vibrations are experiment and spacecraft fans and pumps, motion of centrifuges, and thruster firings. With a crew onboard to conduct experiments, additional vibrations can result from crew activities. The combined acceleration levels that result from the quasi-steady and vibratory contributions are generally referred to as the "microgravity environment of the spacecraft".

Independently from the type of convection both MAC and SMAC methods require staggered grids to guarantee reliable coupling of velocity and pressure (see Fletcher [2] for further details dealing with this aspect).

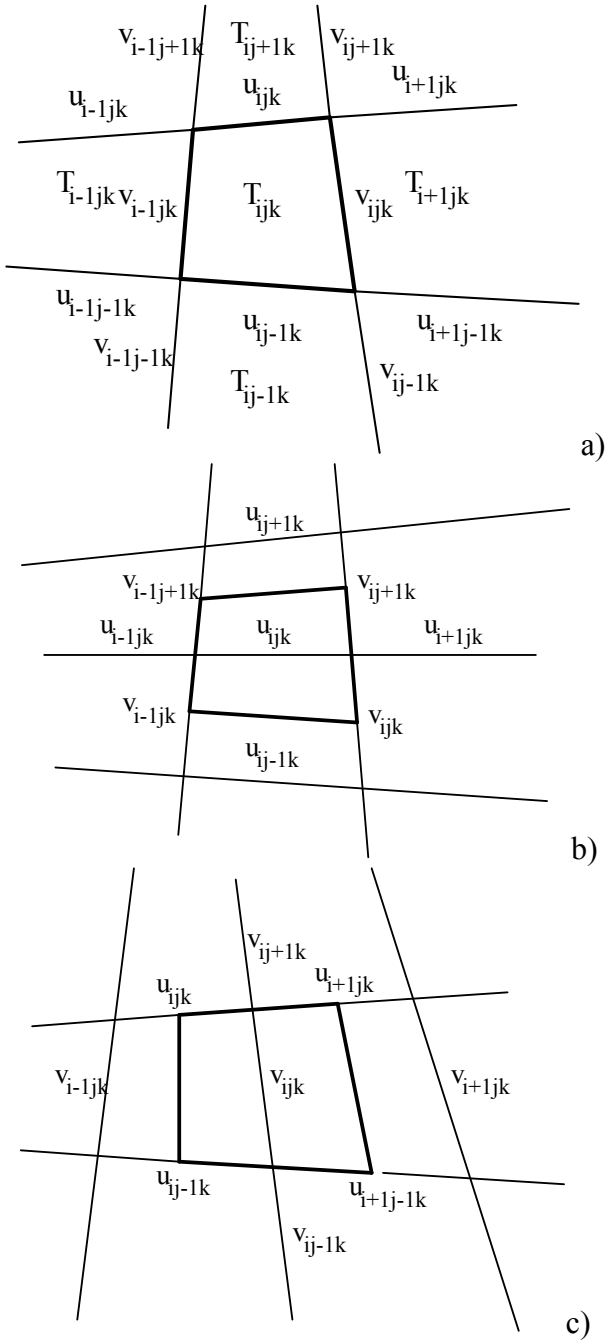

Figs. 1: Staggering for the different variables: the figures show the collocation of temperature and velocity components in the x-y plane (u and v are the velocity components along x and y respectively, the i and j subscripts indicate the relative position along x and y of the nodal values).

Staggering means that the velocity components are computed on the faces of the control-volumes/computational-cells used for pressure, temperature and concentration (these quantities occupy the center of such volumes) i.e. that the control-volumes/computational-cells used for the velocity components are shifted with respect to the one used for pressure, temperature and/or concentration. Figs. 1 show some examples.

The numerical schemes for the spatial discretization of the equations (central differences, upwind schemes, etc.) are no longer discussed in the present paper (it is out of the scope of the present analysis; the reader will find all the details in the excellent books of Fletcher [2]; Hirsch [14] and Deville et al. [15] that are entirely devoted to such aspects).

Rather, in the spirit of the article, the available space is devoted herein to the discussion of some special computational problems that arise when flows with free fluid/fluid interfaces (Marangoni, buoyancy and/or mixed conditions) and/or solid/liquid fronts are considered.

The existence and numerical treatment of momentum, thermal or solutal boundary layers and of vorticity singularities must be regarded as critical issues for the appropriate simulation of these flows. In particular, on one hand, the boundary layers require special care for mesh generation and grid convergence (i.e. for obtaining a grid-independent solution); on the other hand, the presence of numerical singularities introduces additional need for focusing on conditions that make the problem well-posed from a computational point of view.

3.3 NUMERICAL TREATMENT OF BOUNDARY LAYERS

Grid quality is a critical factor for the study of problems concerning Marangoni and buoyancy flows (pure or mixed) and of their steady states, stability properties and possible bifurcations. The complexity of the flow field and the large number of parameters involved require very accurate computations to predict the behavior of the system.

This is particularly true when the flow is characterized by the presence of some regions (hereafter referred to as boundary layers) where extremely steep gradients of velocity and/or temperature and/or concentration are present.

In these cases a larger number of computational points must be used in these portions of the domain to locally enhance the resolution. These points are generally distributed according to stretching functions that allow gradual, somehow smooth increase of the density of points along a given direction. This smooth increase has a twofold purpose: it is required for linking regions where normal resolution is necessary (fixed spatial step) with the aforementioned boundary layers as well as to avoid numerical instabilities; it is known, in fact, that step changes in the points distribution could cause serious problems in terms of stability of the computational algorithm.

In the following, for the sake of simplicity and for educational purposes one dimensional stretching functions are considered. Among other things, it is worthwhile to point out how these functions have enjoyed a widespread use in literature owing to simplicity and efficiency in the treatment of problems where strong gradients occur. For these reasons they are briefly discussed in the following as well.

In these functions the dependent and independent variables are usually expressed in normalized form. For a one-dimensional stretching function applied along a segment AB, the appropriate normalized independent variable varying within the range [0,1] along the aforementioned segment is denoted herein by η ($\eta=0\rightarrow A$, $\eta=1\rightarrow B$).

A possible one-dimensional stretching function is (see Fletcher [2])

$$s = \wp\,\eta + (1-\wp)\left\{1 - \frac{\tanh\left[Q(1-\eta)\right]}{\tanh Q}\right\} \tag{42}$$

where $\wp$ and Q are the parameters controlling grid points distribution ($\wp$ effectively provides the slope of the distribution close to $\eta=0$; Q controls the departure from the linear s versus η; small values of Q cause small departures from linearity; however, also if $\wp$ is close to unity the departure from linearity is small).

Then the grid cells can be distributed along the direction ξ according to simple laws such as:

$$\xi=\xi_A+s(\xi_B-\xi_A) \tag{43}$$

where ξ is the direction perpendicular to the boundary layer and ξ_A and ξ_B (i.e. ξ_B-ξ_B) characterize its width.

The choice of the proper values of $\wp$ and Q (or of other similar parameters if other categories of stretching functions are used) ensuring rapid solution convergence when the number of points is increased, is usually not trivial and requires extensive numerical experimentation.

Also, the directions (ξ) along which the stretching process should be applied are not a priori data of the problem and require numerical experimentation and iterative procedures (first computations with coarse and uniform grids must be carried out, then critical information for mesh generation and points clustering is gained from the preliminary computations).

A first step towards such a critical knowledge, however, is also represented by the Order of Magnitude Analysis (OMA) whose general formulation was derived by Napolitano (see, e.g., Russo and Napolitano [16]) and applied to Marangoni, buoyancy and combined free convection.

The aforementioned analysis, in fact, allows the individuation of the ranges of the non-dimensional characteristic numbers (defined in paragraphs 2.1 and 2.2) and of the conditions for which boundary layers are present. The knowledge of the nature (momentum, thermal, solutal) and of the scale factors governing the evolution of the aforementioned layers is propaedeutical to the appropriate choice of the regions and directions where mesh stretching is necessary as well as to the definition of the related stretching functions.

Table I: Governing equations and Order of Magnitude Analysis

Pr	Sc	χ	Governing equation
$\leq O(1)$	$\leq O(1)$	1	Momentum
$>O(1)$	$\leq O(1)$	Pr	Energy
$\leq O(1)$	$>O(1)$	Sc	Species
$>O(1)$	$>O(1)$	Max{Pr, Sc}	Energy or Species

Table II: Length scale factor and velocity scaling

Test on	ℓ	Velocity scaling
$\chi Re \leq O(1)$	1	V_{Ma}
$\chi Re > O(1)$	$(\chi Re)^{-1/3}$	$V_{Ma}(\chi Re)^{-1/3}$
$\chi Gr \leq O(1)$	1	V_g
$\chi Gr > O(1)$	$(\chi Gr)^{-1/4}$	$V_g(\chi Gr)^{-1/2}$

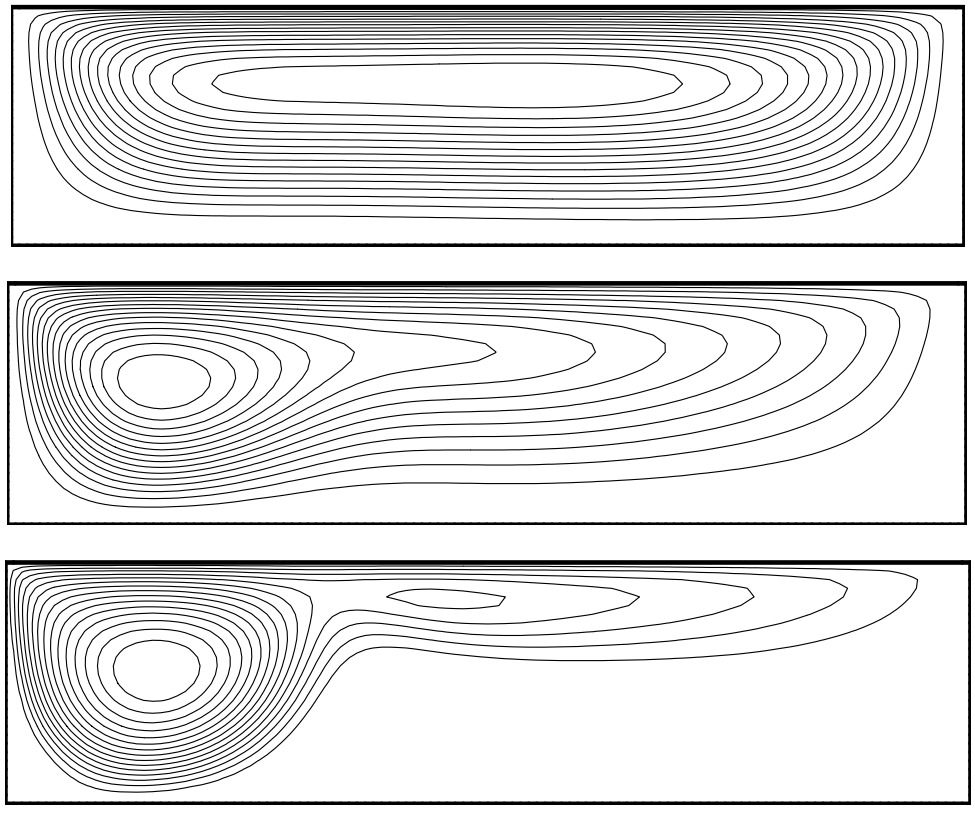

Figs. 2: Structure of pure Marangoni convection for Pr=0.01 (Silicon) and open cavity with aspect ratio A=4 (cold and hot sides on the left and on the right of each frame respectively, upper and lower boundaries with adiabatic conditions): (a) Ma=10, (b) Ma= 100, (c) Ma=1000 (Ma based on the width of the cavity).

The results of the Napolitano's OMA are summarized in Tables I and II (the case of compositionally homogeneous media is evidently obtained by formally setting Sc=0).

In Table II ℓ is a length scale factor at most of order one: if $\ell=1$ no boundary layers are present for the considered phenomenon, if $\ell\neq1$ boundary layers exist and their thickness scales according to ℓ.

Consider for instance the case of pure thermal Marangoni flow (Sc=0) and very small value of the Prandtl number (Pr<<1, e.g. a liquid metal or a semiconductor melt). For this case Table I shows that existence of boundary layers is possible with respect to momentum and gives χ=1. Correspondingly in Table II, two cases are possible Re≤O(1) with $\ell=1$ and Re>O(1) with $\ell=(Re)^{-1/3}$. In the second case (it is the usual situation arising in material processing) the existence of a boundary layer is predicted with thickness changing according to $(Re)^{-1/3}$ (as Re increases it becomes thinner).

This means that for the case of liquid metals and semiconductor melts non-uniform grids stretched close to the free surface should be used.

This zone plays a critical role in the computations since therein a Marangoni boundary layer is present with extremely steep radial gradients of velocity induced by the driving force acting on the free surface. Direct numerical experimentation shows that this is particularly true for very large values of the Re number ($O(Ma)>10^2$) as shown in Figs. 2.

The results provided by the OMA in this case become even more important if one considers that, on the basis of Table I, no thermal boundary layers should be present (or if present should be weak): "Momentum" in the last column means, in fact, that the prominent features of the field are related to this quantity and that other (thermal and/or solutal) effects should be negligible in terms of steepness of the related gradients (hereafter the word "prominent" is used to denote only the features of the TFD field that exhibit steep gradients). From a physical point of view the absence of thermal boundary layers follows from the large thermal diffusivity of liquid metals that spreads thermal gradients over wide regions.

These are the reasons why, for relatively small values of the Marangoni number (Ma=O(10)) grid refinement studies simply show that for the case of liquid metals (Pr<<1), the numerical simulation of the problem is not adversely affected by the use of uniform grids. For this case in fact, in the light of the aforementioned arguments, both momentum and thermal boundary layers are absent or weak and grid convergence is achieved quite easily (see, e.g., Lappa [17]).

As anticipated, when Ma becomes large stretching functions clustering the computational points close to the free surface should be chosen. Since the isotherms tend to be compressed by the flow towards the cold wall, some points should also be accumulated close to this boundary.

Strong thermal gradients, however, are expected for the case of high Prandtl number (transparent and organic) liquids; extensive numerical experimentation shows that for Pr>>1, in fact, very thin thermal boundary layers appear close to the heated (or cooled) sides. For this case special care (non-uniform grids and/or regularization conditions) has to be provided in order to capture the detailed structure of the thermal and velocity fields (in particular the velocity distribution close to the corners) and to obtain grid-convergence (see the next sub-paragraph for this subject).

This situation is predicted in principle by the OMA results in Tables I and II. In fact, for Pr>O(1) the prominent features of the field are related to its thermal structure ("Energy" appears in the last column of Table I); in this case χ=Pr and the thickness of the thermal boundary layers scales according to $\ell=(Pr\cdot Re)^{-1/3}=(Ma)^{-1/3}$. Such a behavior is qualitatively confirmed by the numerical results shown in Figs. 3. The temperature fields clearly exhibit bands close to the heated (or cooled) walls where the isotherms tend to be compressed. The width of these layers is reduced as Ma increases, leading to an increasing demand for points in these regions (see, e.g., Fig. 4).

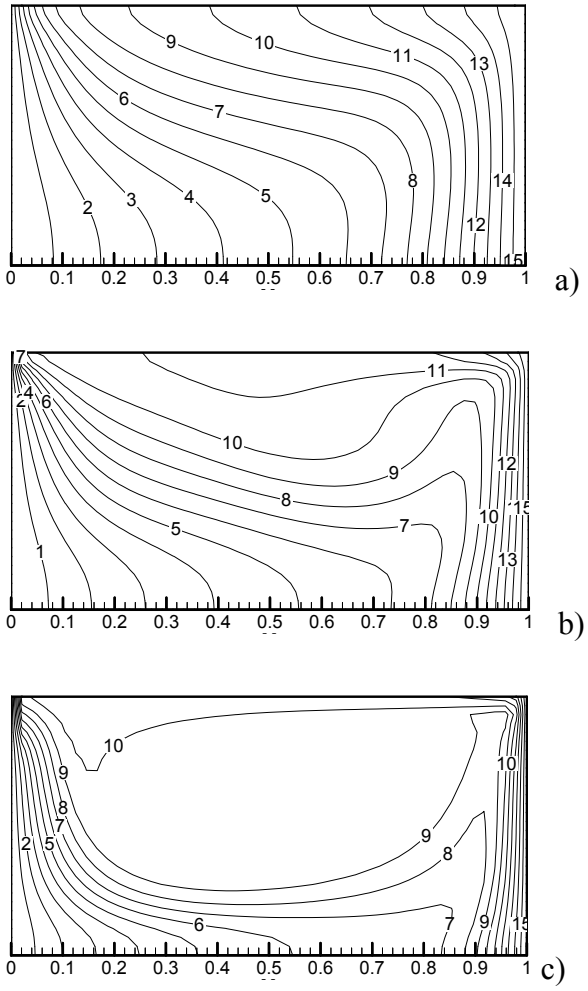

Figs. 3: Open cavity problem, Pr=15, A=2.0, temperature distribution, cold wall on the left side, hot wall on the right side, upper and lower boundaries with adiabatic conditions: (a) $Ma=10^3$, (b) $Ma=10^4$, (c) $Ma=10^5$. (level 1→T=0.06, level 15→T=0.94; Δlevel=0.06)

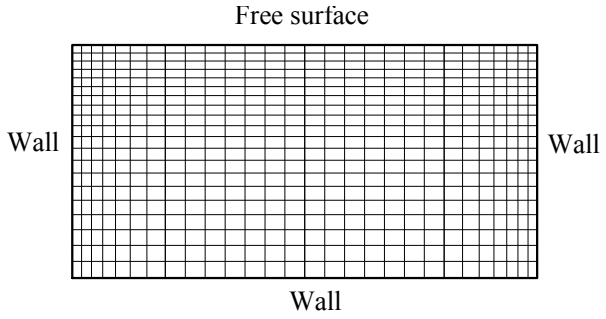

Fig. 4: Example of grid for the open cavity problem obtained combining one-dimensional stretching function along x and y ($\wp$=2 and Q=1).

3.4 VISCOUS SINGULARITIES AND REGULARIZATION FUNCTIONS

Confined Marangoni flows (for instance in open cavities or in liquid bridges) are characterized by the presence of a singularity where free and solid surfaces meet. The singularity is particularly evident if one considers the vorticity distribution (see Fig. 5).

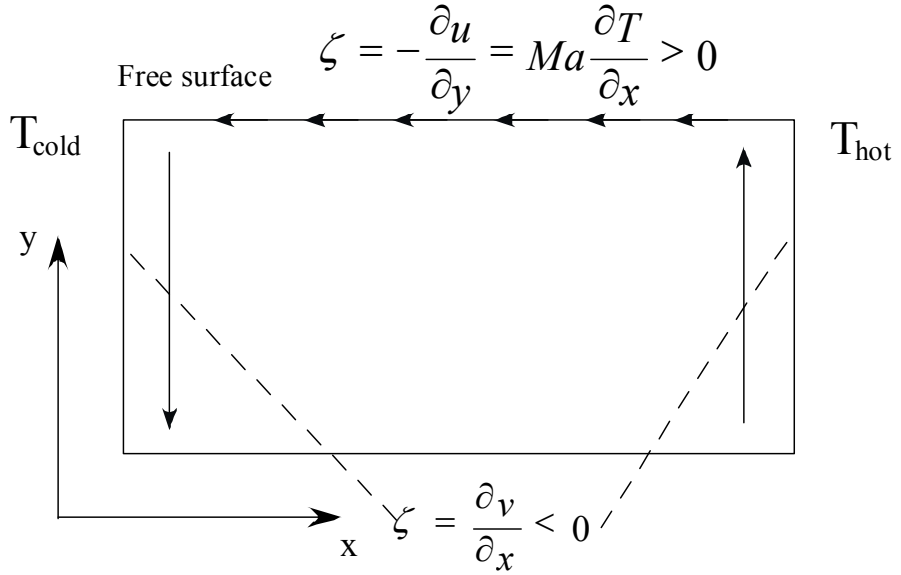

Fig. 5: Sketch of the conditions responsible for the viscous singularities (u and v are the velocity components along x and y respectively).

Since the vorticity is given by $\zeta=\partial v/\partial x-\partial u/\partial y$, it reduces to $\zeta=-\partial u/\partial y>0$ along the free surface (where v=0) which behaves as a source of positive vorticity. The no-slip conditions on the solid boundaries generate instead a negative vorticity $\zeta=\partial v/\partial x<0$ (u=0). Accordingly, there is a jump discontinuity for the vorticity in the surface corners (in practice it is a jump discontinuity for the shear stress from which the more proper denomination of "viscous singularity").

This singularity is very important as it affects the flow at any contact free surface/solid boundary. It can seriously jeopardize the physical consistency of the numerical solution and also retard convergence, and sometimes lead to oscillations that may result in grid-divergence. In the light of these arguments, a physically relevant modeling of the contact free surface/solid boundary appears as a pre-requisite of any numerical simulation.

In practice, any computational treatment of these flows must filter this singularity: depending on the circumstances this task can be accomplished implicitly by using finite precision methods or explicitly by modifying the boundary conditions of the problem (the so-called regularization, Kasperski and Labrosse [18]).

Usually such a regularization is not necessary for low Prandtl number fluids (Pr<<1) since in this case the singularity is implicitly by-passed by the finite precision spatial discretization that is based on local approximation of the derivatives. If the problem, for instance, is solved with the very commonly employed, second order in space, finite-difference scheme, the resulting numerical solution will not be affected by any singular contribution thanks to the filtering properties of the local approximation of the differential operators.

In practice, the finite difference schemes automatically act to regularize, through some filtering mesh-dependent function, the initially singular formulation. The numerical solution converges, asymptotically with the mesh refinement, toward the solution of a continuous problem (Kasperski and Labrosse [18]).

On the contrary the explicit regularization is a critical requirement, for high Prandtl number liquids (Pr>1) and in particular for large values of the Marangoni number. For these cases grid-convergence cannot be obtained or occurs only if very dense (often prohibitive for three-dimensional simulations) computational meshes are used.

As previously explained, for these liquids strong thermal boundary layers appear close to the heated (or cooled) boundaries with thickness scaling according to $\ell=(\mathrm{Pr}\cdot\mathrm{Re})^{-1/3}=(\mathrm{Ma})^{-1/3}$.

The boundary layer close to the cold wall in particular is responsible for the presence of a large number of isotherms confined in a very thin region close to the free surface. Such a compression in turn is responsible (via the surface Marangoni boundary condition) for the presence of a velocity peak therein. Often the magnitude

of the velocity in this point diverges as the mesh is refined.

These are sufficient reasons for considering the explicit treatment of the singularity as essential regarding the physical relevance of the results.

The regularization approach, rather than relying on the intrinsic filtering properties of the numerical scheme (that in this case are not sufficient), tries to get an explicit regular continuous formulation of the problem by an appropriate modeling of the underlying physical regularity.

The physical consistency requires in particular that experiments performed with a frozen geometry should exhibit small scales, on the free surface, in the vicinity of the solid boundaries within which the physical regularity is satisfied at the scale of the continuos medium. From a mathematical point of view, this condition is achieved if the Marangoni stresses vanish at the solid walls while keeping a continuous behavior. Following the excellent approach of Kasperski and Labrosse [18] all these element together can be taken into account, in a very simplified way, by introducing the regularizing function (the walls are supposed to be located at x=±1)

$$f_n(x) = \left(1 - x^{2n}\right)^2 \tag{44}$$

in the boundary conditions (20) i.e.:

$$\frac{\partial \underline{V}}{\partial n} = -Ma\ f_n(x)\ \underline{\nabla_S} T \tag{45}$$

where n is the so-called filtering parameter.

A measure of the filtering length, the distance over which the regularization acts, is defined by δ(n) such that $f_n(x=1-\delta(n))=0.95$, which leads to

$$\delta(n) = 1 - 0.0253^{1/2n} \tag{46}$$

i.e. the higher is n, the smaller is the filtering scale.

This length scale behaves as a new free parameter with respect to which the convergence of the results must be assessed.

It must be decreased (increasing n) until an asymptotic behavior appears that is a good indication of the physical relevance of the model and of the obtained flow. In other words for a given problem, preliminary convergence tests have to be carried out for the appropriate choice of n. These tests generally show that the appropriate n behaves as an increasing function of the Marangoni number.

In the case of solidification problems (non-frozen geometries), the use of the regularization condition (44) near the melt/solid fronts follows directly from the physical behavior of the liquid therein; the viscosity, in fact, must tend to an infinite value on the freezing front (i.e. Ma→0 locally, see, e.g., Lappa and Savino [19]).

4. REFERENCES

[1] M..J.B. Rogers, G.L. Vogt, M.J. Wargo, (1997), "Microgravity: A Teacher's Guide", EG-1997-08-110-HQ, NASA publication (1997).i

[2] C.A.J. Fletcher, (1991) "Computational techniques for fluid-dynamics", (Springer Verlag, Berlin, 1991)

[3] H.C. Kuhlmann, "Some scaling aspects of thermocapillary flows", Microgravity Quarterly, 5, (1995), 29-34.

[4] A. Rybicki, J.M. Florian, "Thermocapillary effects in liquid bridges. I. Thermocapillary convection", Phys. Fluids, 30, (1987), 1956-1972.

[5] P.M. Gresho, "Incompressible fluid dynamics: some fundamental formulation issues", Ann. Rev Fluid Mech., 23, (1991), 413-453.

[6] B. Farouk, T. Fusegi, "A coupled solution of the vorticity-velocity formulation of the incompressible Navier-Stokes equations", Int. J. Numer. Meth. Fluids 5, (1985), 1017-1034.

[7] F.H. Harlow and J.E. Welch, "Numerical calculation of time-dependent viscous incompressible flow with free surface", Phys. Fluids, 8, (1965), 2182-2189.

[8] P.M. Gresho, R.T. Sani, "On pressure boundary conditions for the incompressible Navier-Stokes equations", Int. J. Numer. Meth. Fluids, 7, (1987), 1111-1145.

[9] M. Lappa, "Strategies for parallelizing the three-dimensional Navier-Stokes equations on the Cray T3E ", Science and Supercomputing at CINECA, 11, (1997), 326-340.

[10] M. Lappa and R. Savino, "Parallel solution of the three-dimensional Marangoni flow instabilities in liquid bridges"; Int. J. Numer. Meth. Fluids, 31, (1999), 911-925.

[11] G.Z. Gershuni, E.M. Zhukhovitskii, Yu. S. Yurkov, (1982), "Vibrational thermal convection in a rectangular cavity", Izv. Akad. Nauk SSSR Mekh. Zhidk. Gaza, 4: 94-99.

[12] G.Z. Gershuni, E.M. Zhukhovitskii, "Vibrational thermal convection in zero gravity", Fluid. Mech.-Sov. Res. 15, (1986), 63-84.

[13] G.Z. Gershuni, D.V. Lyubimov, (1998), "Thermal Vibrational Convection", Wiley&Sons (1998).

[14] C. Hirsch, (1994), "Numerical computations for internal and external flows", John Wiley and Sons.

[15] M.O. Deville, E.H. Mund, P. F. Fischer, "High-order methods for incompressible fluid flow", Cambridge University Press, (2002), 1-528.

[16] G. Russo, L.G. Napolitano, (1984), "Order of Magnitude Analysis of unsteady Marangoni and Buoyancy free convection", 35th Congress of the International Astronautical Federation, October 7-13, 1984, Lausanne, Switzerland.

[17] M. Lappa, "Three-dimensional numerical simulation of Marangoni flow instabilities in floating zones laterally heated by an equatorial ring", Phys. Fluids, 15 (3), (2003), 776-789.

[18] G. Kasperski, G. Labrosse, "On the numerical treatment of viscous singularities in wall-confined thermocapillary convection", Phys. Fluids, 12(11), (2000), 2695-2697.

[19] M. Lappa, R. Savino, "3D analysis of crystal/melt interface shape and Marangoni flow instability in solidifying liquid bridges", J. Comput. Physics 180 (2), (2002), 751-774.